

In-Plane Orientation in Poly(amic acid)s during Thermal Imidization

Shin`ya MORINO[†] and Kazuyuki HORIE*

Photofunctional Chemistry Division, Research Laboratory of Resources Utilization, Tokyo Institute of Technology, 4259 Nagatsuta, Midori-ku, Yokohama 226-8503, Japan

**Department of Chemistry and Biotechnology, Graduate School of Technology, The University of Tokyo, 7-3-1 Hongo, Bunkyo-ku 113-8656, Japan*

(Received March 5, 1999)

ABSTRACT: Refractive indices of in-plane and out-of-plane directions were measured for a poly(amic acid) (PAA) synthesized from biphenyltetracarboxylic dianhydride and *p*-phenylenediamine and PAA synthesized from biphenyltetracarboxylic dianhydride and *p,p'*-diaminodiphenylether. Depth dependence of in-plane orientation was observed for both PAAs. The degree of in-plane orientation is larger around the air/film interface than the film/substrate interface. Factors which contribute to increase in average refractive index are solvent evaporation, thermal imidization and dense packing during heating. Solvent evaporation is dominant for curing at temperatures below 100°C, thermal imidization is dominant for curing at temperatures from 100°C to 200°C and change in packing becomes important for curing at temperatures above 200°C.

KEY WORDS Polyimides / In-Plane Orientation / Birefringence / Thermal Imidization / *m*-Line Method / Polymer Thin Films /

In recent years, in-plane orientation of polyimides (PIs) has been of interest because of large birefringence.^{1–7} This birefringence can be applied to optical devices such as waveplates,² polarizers and so on. Effort was also made to apply this material for a compensator of liquid crystal displays.³

The stiffness of PI main chain affects physical properties and in-plane orientation.^{2–6} This stiffness is governed by the chemical structure of polyimides. Degree of in-plane orientation depends on mismatch of thermal expansion coefficient.² Biaxial drawing takes place when volume loss occurs during solvent evaporation and imidization. Polyimide films are surrounded by superstrates (air in typical cases) and substrates and are asymmetric along the out-of-plane direction. It is expected to observe asymmetry in optical properties along the out-of-plane direction.

Optical properties of poly(amic acid)s (PAA) and polyimides (PI) reflect density, chemical composition and degree of orientation. For example, charge transfer absorption is observed for some polyimides, which shows the packing structure of the polyimide main chain. Because the refractive index, one of optical properties, is measured with high accuracy (at least 4 digits), it could be a useful method to investigate changes in physical and chemical properties.

In the present paper, refractive index of in-plane and out-of-plane directions are measured during thermal imidization of some poly(amic acid)s. Depth dependence of refractive indices and degree of in-plane orientation are discussed.

EXPERIMENTAL

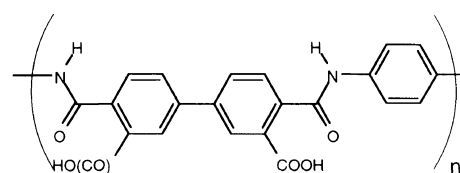
Preparation of Poly(amic acid) Films

Figure 1 shows the chemical structures of poly(amic acid)s used in this study. Poly(amic acid)s, PAA(BPDA/PDA), synthesized from biphenyltetracarboxylic dianhydride and *p*-phenylenediamine, and PAA(BPDA/

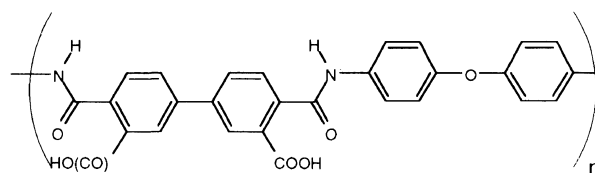
ODA) synthesized from biphenyltetracarboxylic dianhydride and *p,p'*-diaminodiphenylether were prepared by the conventional manner as mixing equal molar of a dianhydride and a diamine in a suitable solvent such as *N,N'*-dimethylacetamide (DMAc). The mixtures were sealed and stirred for one day, reprecipitated from methanol, and dried at room temperature for one day. The resulting PAAs were dissolved into DMAc again and spincoated (500 rpm for 30 s) on fused silica substrates, and dried under vacuum at 50°C for one day. Film thickness was set at *ca.* 5 μm.

Refractive Index Measurements

Refractive index measurements were carried out by an *m*-line method.^{13–15} Figure 2 depicts the measurement system. Films on fused silica substrates work as slab waveguides. Waveguided modes consist of two orthogonal modes, TE and TM. TE modes have a parallel electric component to the film plane, and TM modes have a parallel magnetic component to the film plane. Both



PAA(BPDA/PDA)



PAA(BPDA/ODA)

Figure 1. Chemical structures of poly(amic acid)s used in this study.

[†] To whom correspondence should be addressed.

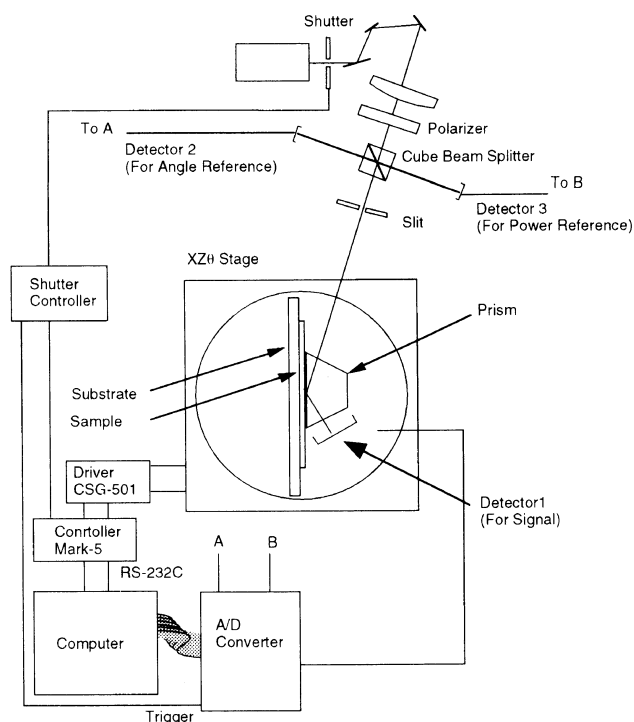


Figure 2. Setup for refractive index measurements by the m -line method.

modes are selected by rotating the plane of polarization of incident laser beam at 632.8 nm from a He-Ne laser. By using a prism coupler, waveguided modes were excited. Effective refractive indices were measured for each mode by measuring the incident angle to the prism plane when waveguided modes were excited most effectively. The intensity of waveguided light was determined with the intensity of scattering light from the waveguide. Effective refractive indices were calculated using eq 1 written as,

$$n_{\text{eff}} = n_p \sin\left(\alpha + \sin^{-1}\left[\frac{n_{\text{air}}}{n_p} \sin\{\theta_{\text{obs}}\}\right]\right) \quad (1)$$

where n_{eff} is the effective refractive index, n_p , n_{air} , and n_{film} are refractive indices of the prism, the air, and films, respectively, and α is the angle of the prism, and θ_{obs} is the incident angle to the prism. The relationship between the effective refractive index, film thickness, W , and the refractive index of the film, n_{film} , are described by the following eigen value equation,

$$k_0 W \sqrt{n_{\text{eff}}^2 - n_{\text{film}}^2} - \Phi_{\text{sub}} - \Phi_{\text{air}} = m\pi \quad (2)$$

$$\Phi_i = \arctan\left(\zeta \left(\frac{n_{\text{film}}}{n_i}\right)^a \sqrt{\frac{n_{\text{eff}}^2 - n_i^2}{n_{\text{film}}^2 - n_{\text{eff}}^2}}\right)$$

i = air, sub

where k_0 is the wavenumber of the incident laser beam in vacuum, an integer, m , is the mode number, and n_{sub} is the refractive index of the substrate. n_{TE} and n_{TM} represent the refractive index of in-plane and out-of-plane orientation of films, respectively. For TE modes, $\zeta = 1$, $a = 0$. For TM modes, $\zeta = (n_{\text{TE}}/n_{\text{TM}})$, $a = 2$. n_{TE} , n_{TM} , and W were calculated by least square fitting using eq 1, 2 with appropriate values for n_p , n_{air} , n_{sub} , and α .

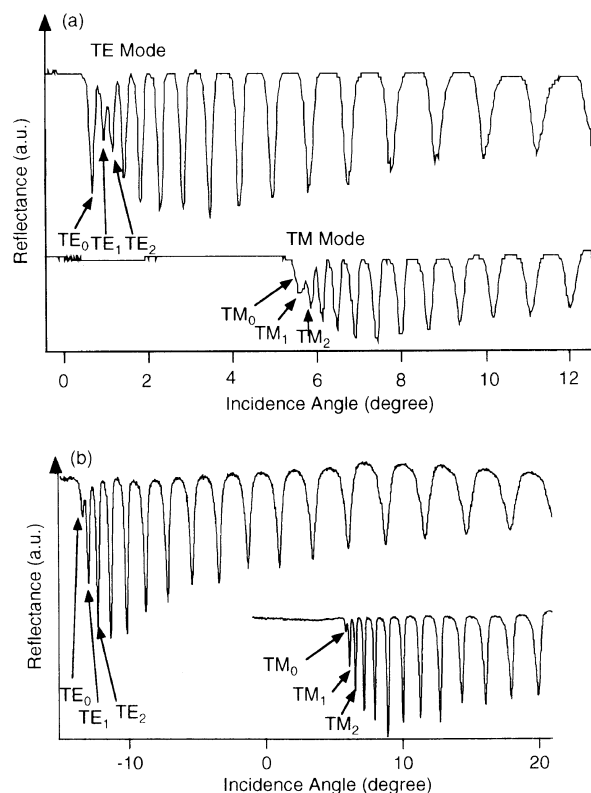


Figure 3. m -Line spectra of PAA(BPDA/PDA) before annealing (a) and after annealing at 160°C (b).

Refractive Index Measurements During Stepwise Thermal Imidization

Refractive indices were measured for PAA films of various degrees of thermal imidization by heating at temperatures from 50°C to 350°C for 2 h under vacuum successively. Refractive indices were measured after heating at each temperature.

Determination of Degree of Imidization

Free-standing PAA films fabricated in the same manner as above were used for IR spectra measurements. The degree of imidization was obtained from IR absorbance of imide carbonyl group at 1780 cm^{-1} with the internal standard of IR absorbance of a benzene ring at 1515 cm^{-1} .

RESULTS AND DISCUSSION

Figure 3 shows the typical m -line spectra of PAA-(BPDA/PDA) before annealing and after annealing at 160°C. This result for the TE mode cannot be analyzed with the assumption of no depth dispersion of refractive index. As shown in Figure 3(a), m -line spectra of PAA(BPDA/PDA) show unusual behavior that the TE_0 peak is stronger than TE_1 peak, and the interval between TE_0 and TE_1 is wider than that between TE_1 and TE_2 , though this behavior is not observed for TM modes. For step-index planar waveguides, coupling efficiency from a prism to waveguide, calculated from the dip in reflectance, is larger for modes of higher order because evanescent field is stronger for waveguided modes of higher order, and intervals between the neighboring modes are smaller for modes of lower order. Such behavior

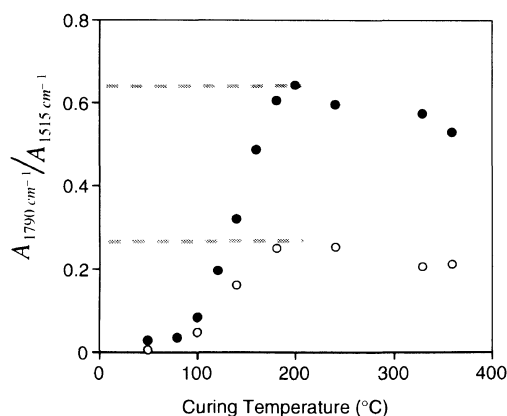


Figure 4. Curing temperature dependence of the conversion of imidization. Ratio of absorbance at 1790 cm^{-1} to that at 1515 cm^{-1} is plotted for PAA(BPDA/PDA) (●) and PAA(BPDA/ODA) (○).

was not observed for annealed PAA(BPDA/PDA) film as shown in Figure 3(b). Therefore annealed film can be treated as a step-index waveguide. Figure 3(a) suggests that there is strong depth dependence of refractive index, and is explained as follows. Refractive index of PAA films is larger around an air/waveguide interface, which results in total reflection of waveguided light in the middle of the film, and reduces the effective thickness for the TE_0 mode. TE_0 mode is guided around an air/waveguide interface, and intensity of evanescent field is stronger than the TE_1 mode at the air/film interface, which increases coupling efficiency. TM_0 modes for both films were very weak, which shows that this mode is well-guided, and intensity of evanescent wave is very weak. This suggests lower refractive index at the air/film interface than that at the film/substrate interface. From these results, we conclude that in-plane orientation proceeds faster around an air/film interface than film/substrate interface. We had expected that strong orientation around film/substrate interface would arise from the anchoring of PAA molecules on substrates as shown in liquid crystal/substrate interfaces. But substrates do not play an important role except of binders of films.

To calculate refractive indices, the TE_0 mode was ignored to eliminate the effect of the depth dependence of refractive index. Refractive indices were obtained as 1.651 for n_{TE} and 1.597 for n_{TM} of PAA(BPDA/PDA). Values were also 1.634 for n_{TE} and 1.602 for n_{TM} for PAA(BPDA/ODA). Film thickness was also obtained by m -line measurements as *ca.* $5\text{ }\mu\text{m}$ for both films. Thickness dependence of in-plane-orientation has been investigated, and reported thinner than $10\text{ }\mu\text{m}$ required for strong in-plane orientation.^{9,12} Both PAA films show birefringence between in-plane and out-of-plane directions. In-plane orientation of polyimides arises from biaxial drawing caused by volume-loss during imidization,^{1,2,6} which occurs because films are bounded to substrates. The origin of volume loss for PAA films is evaporation of a casting solvent. Evaporation of the solvent is faster around the air/film interface than around the film/substrate interface, which results in the depth dependence of in-plane orientation. The same behavior was observed for m -line spectra of PAA(BPDA/ODA).

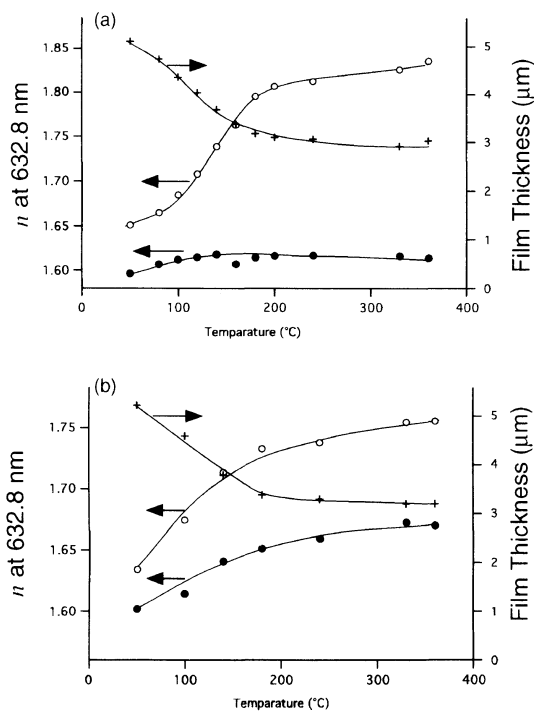


Figure 5. Curing temperature dependence of refractive indices of out-of-plane direction (●) and in-plane direction (○), and film thickness (+) for PAA(BPDA/PDA) (a) and PAA(BPDA/ODA) (b).

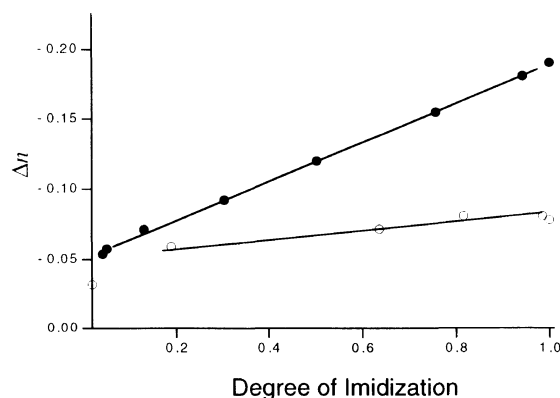


Figure 6. Birefringence as a function of imidization for PAA(BPDA/PDA) (●) and for PAA(BPDA/ODA) (○).

Figure 4 shows estimation of the degree of imidization. The ratio of absorbance at 1780 cm^{-1} to that at 1515 cm^{-1} saturated around 200°C , caused by the fact that the absorption at 1780 cm^{-1} includes absorption which arises from acid anhydride whose formation was confirmed by IR absorption band at 1850 cm^{-1} . Here we approximated that imidization finished at about 200°C .

Figure 5 shows curing temperature dependence of n_{TE} , n_{TM} and film thickness obtained by m -line measurements. Birefringence, $\Delta n = (n_{\text{TM}} - n_{\text{TE}})$, calculated from the obtained values in Figure 5 is plotted as a function of the conversion of imidization in Figure 6. Values of birefringence are negative because of negative anisotropy of in-plane orientation. The birefringence of PAA(BPDA/PDA) shows linear relationship with the conversion of imidization, though that of PAA(BPDA/ODA) shows only slight increase with the conversion of imidization larger than 0.6. Similar behavior was reported for tensile

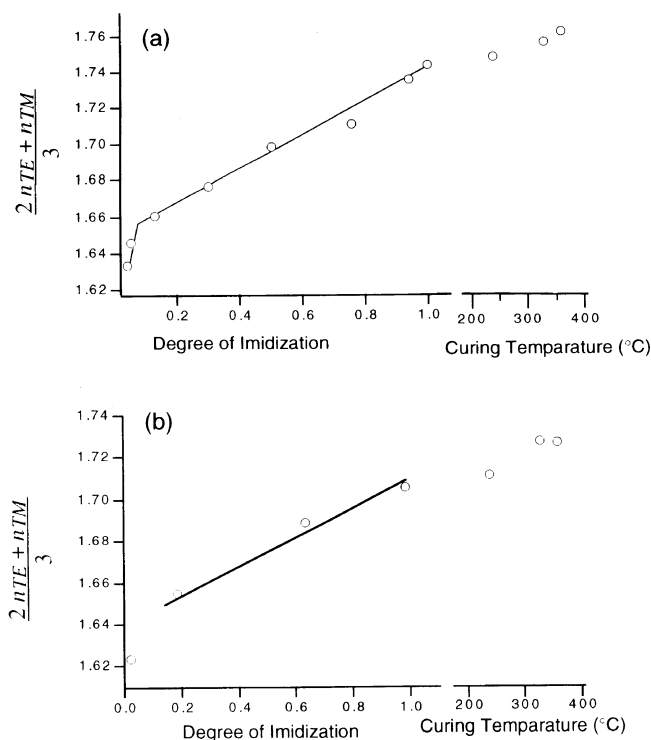


Figure 7. Conversion dependence of average refractive index for PAA(BPDA/PDA) (a) and PAA(BPDA/ODA) (b).

strength on axial drawing of the same poly(amic acid)s. The bent in main chain at the ether group of ODA may thus cause sliding between polymer chains, which weakens the axial ordering of poly(amic acid)s.

The depth dependence of in-plane orientation observed for PAA films was not observed for films cured above 120°C. Because thickness decreased and imidization proceeds all depth regions, the TE_0 mode is not affected by the depth dependence of in-plane orientation.

For detailed analysis of refractive index and thickness changes, the average refractive index of $[(2n_{TE} + n_{TM})/3]$ is plotted as a function of the degree of imidization in Figure 7. In the figure, the results for temperatures higher than 240°C are plotted as a function of curing temperature because conversion of imidization was assumed to be unity. For PAA(BPDA/PDA) rapid increase in average refractive index for degree of imidization from 0 to 0.05, and slow increase for conversion of imidization larger than 0.05 were observed. According to the Lorentz-Lorenz equation, refractive index is determined by molar refraction and density. Molar refraction is affected by chemical composition, which corresponds to solvent content and degree of thermal imidization. Change in density was observed as thickness change. The rapid increase is induced by the evaporation of the casting solvent. This is dominant for

curing below 100°C which corresponds to the degree of imidization of 0.05. The slow increase is due to thermal imidization. Birefringence continued to increase for curing above 200°C. This reflects increase in density because of dense packing of aromatic imide groups. Similar behavior was observed for PAA(BPDA/ODA).

CONCLUSION

Refractive indices of in-plane and out-of-plane directions were measured for poly(amic acid)s, PAA(BPDA/PDA) and PAA(BPDA/ODA). Depth dependence of in-plane orientation was observed for both PAAs. Degree of in-plane orientation is smaller around the film/substrate interface than around the air-film interface, though films are drawn because of being bound to substrates. Solvent evaporation, thermal imidization and dense packing contribute to increase in average refractive index during thermal imidization. Solvent evaporation is dominant for curing below 100°C, thermal imidization from 100°C to 200°C, and change in packing becomes important for curing above 200°C.

Acknowledgments. This work is partly supported by a grant-in-aids for Scientific Research (06555287) from the Ministry of Education Science, Sports and Culture of Japan. The authors thank Dr. M. Hasegawa in Toho University for helpful discussion.

REFERENCES

1. T. P. Russel, H. Guggler, and J. D. Swalen, *J. Polym. Sci., Polym. Phys. Ed.*, **21**, 1745 (1983).
2. S. Ando, T. Sawada, and Y. Inoue, in "Polymeric materials for Microelectronic Applications," H. Ito, S. Tagawa, and K. Horie, Ed., ACS Symposium Series 579, American Chemical Society, Washington, D.C., 1994, p 283.
3. F. Li, F. W. Harris, and S. Z. D. Cheng, *Polymer*, **37**, 5321 (1996).
4. R. M. Ikeda, *J. Polym. Sci., Polym. Lett. Ed.*, **4**, 353 (1996).
5. M. Hasegawa, T. Matano, Y. Shindo, and T. Sugimura, *J. Photopolym. Sci. Technol.*, **7**, 275 (1994).
6. M. Hasegawa, T. Matano, Y. Shindo, and T. Sugimura, *Macromolecules*, **29**, 7987 (1996).
7. S. Ermer, in "Photosensitive Polyimides," K. Horie, and T. Yamashita, Ed., Technomic Publ. Co., Lancaster, 1995, Chapter 10.
8. L. Lin and S. A. Bidstrup, *J. Appl. Polym. Sci.*, **54**, 553 (1994).
9. M. Ree, Y.-H. Park, K. Kim, C. K. Cho, and C. E. Park, *Polymer*, **38**, 6333 (1997).
10. D. Boese, H. Lee, D. Y. Yoon, J. D. Swalen, and L. F. Tabolt, *J. Polym. Sci., Phys. Ed.*, **30**, 1321 (1992).
11. M. Ree, C. Chu, and M. J. Goldberg, *J. Appl. Phys.*, **75**, 1410 (1994).
12. F. Li, K. Kim, E. P. Savitski, J. Chen, F. W. Harris, and S. X. D. Cheng, *Polymer*, **38**, 3223 (1997).
13. P. K. Tien, *Appl. Opt.*, **10**, 2395 (1971).
14. W. M. Prest and D. J. Luca, *J. Appl. Phys.*, **50**, 6067 (1979).
15. W. M. Prest and D. J. Luca, *J. Appl. Phys.*, **51**, 5170 (1980).